Available online at www.sciencedirect.com
ScienceDirect
International Journal of Solids and Structures 44 (2007) 2802–2819
INTERNATIONAL JOURNAL OF SOLIDS and STRUCTURES
www.elsevier.com/locate/ijsolstr

Corner stress singularities in an FGM thin plate

C.S. Huang *, M.J. Chang

Department of Civil Engineering, National Chiao Tung University, 1001 Ta-Hsueh Road, Hsinchu 30050, Taiwan

Received 7 April 2006; received in revised form 31 July 2006
Available online 1 September 2006

Abstract

Describing the behaviors of stress singularities correctly is essential for obtaining accurate numerical solutions of complicated problems with stress singularities. This analysis derives asymptotic solutions for functionally graded material (FGM) thin plates with geometrically induced stress singularities. The classical thin plate theory is used to establish the equilibrium equations for FGM thin plates. It is assumed that the Young's modulus varies along the thickness and Poisson's ratio is constant. The eigenfunction expansion method is employed to the equilibrium equations in terms of displacement components for an asymptotic analysis in the vicinity of a sharp corner. The characteristic equations for determining the stress singularity order at the corner vertex and the corresponding corner functions are explicitly given for different combinations of boundary conditions along the radial edges forming the sharp corner. The non-homogeneous elasticity properties are present only in the characteristic equations corresponding to boundary conditions involving simple support. Finally, the effects of material non-homogeneity following a power law on the stress singularity orders are thoroughly examined by showing the minimum real values of the roots of the characteristic equations varying with the material properties and vertex angle.

Keywords: FGM thin plates; Stress singularities; Asymptotic solutions; Eigenfunction expansion method

1. Introduction

Functionally graded materials (FGMs) were first produced in Japan in the mid-1980s (Niino and Maeda, 1990). An FGM is a multi-phase material comprised of different material components, such as ceramics and metals, that have various mixture ratios and microstructures. The gradual variation in material composition rather than sharp interfaces, as in the case of multilayered systems (i.e., laminated composites), significantly enhances the thermal and mechanical features of FGMs. Furthermore, FGMs can be designed to meet particular requirements, such as enhanced stiffness, toughness and resistance to corrosion, wear and high temperature, by using materials or material systems with various properties. Consequently, in the last two decades, FGMs have been used in numerous demanding engineering applications including military armor, thermal barrier coating for turbine blades and internal combustion engines and machine tools.

* Corresponding author. Tel.: +886 3 5712121x54962.
E-mail address: cshuang@mail.nctu.edu.tw (C.S. Huang).

0020-7683/$ - see front matter © 2006 Elsevier Ltd. All rights reserved.
doi:10.1016/j.ijsolstr.2006.08.024

An FGM plate can be designed with material properties that vary gradually in the thickness direction, such that the plate is non-homogeneous in that direction only. A plate is a widely used component in practical engineering, and has various shapes. A plate with a reentrant corner or V-notch often shows stress singularities at the corner or vertex. These stress singularities must be considered if analysis is to be of real use. Stress singularity behaviors in a problem must be properly considered to obtain a convergent and accurate numerical solution (Leissa et al., 1993; Huang et al., 2005).

Studies of stress singularities resulting from various boundary conditions in angular corners of plates are limited to homogeneous plates or bi-material plates. Williams (1952a,b) first showed the stress singularities of a thin plate under extension or bending due to various boundary conditions. Based on plane elasticity or classical plate theory, several studies used various approaches to investigate stress singularities at the interface corner of a bi-material plate (Hein and Erdogan, 1971; Bogy, 1971; Rao, 1971; Gdoutos and Theocaris, 1975; Dempsey and Sinclair, 1981; Ting and Chou, 1981). Burton and Sinclair (1986), Huang (2002a,b, 2003, 2004), and McGee et al. (2005) investigated the stress singularities at thick plate corners using different plate theories or various analytical solution techniques. Based on three-dimensional elasticity, Bažant and Estenssoro (1977), Keer and Parihar (1977), Schmitz et al. (1993), and Glushkov et al. (1999) applied different numerical solution techniques to investigate geometrically induced stress singularities at a three-dimensional vertex of a homogenous body. Somaratna and Ting (1986) and Ghahremani (1991) used a finite element approach to study stress singularities in anisotropic materials and composites. Huang and Leissa (in press) developed three-dimensional corner displacement functions for bodies of revolution.

Although geometrically induced stress singularities on an FGM plate have never been investigated, crack-related problems in FGMs have been frequently studied using plane or three-dimensional elasticity theory. Based on plane elasticity, Delale and Erdogan (1983) and Erdogan (1985) employed integral equation techniques to solve crack problems with mechanical loading, whereas Noda and Jin (1993) and Jin and Noda (1993) considered thermal loading. Furthermore, Erdogan and his co-workers (1988, 1991) investigated interface crack problems in bonded FGM plates. Using three-dimensional elasticity, Gu and Asaro (1997) applied an asymptotic solution of crack tip stress and displacement fields for homogeneous materials to examine small crack deflection in brittle FGMs. Gu et al. (1999), Rousseau and Tippur (2002), Kim and Paulino (2002), and Jin and Dodds (2004) applied different finite element techniques to solve various crack problems. Chen et al. (2000) and Yue et al. (2003) utilized the mesh free Galerkin method and boundary element approach, respectively, to solve various crack problems.

This work examines geometrically induced stress singularities for an FGM plate using classical thin plate theory. The equilibrium equations in terms of displacement components on the mid-plane are developed for an FGM thin plate. The in-plane displacement components are coupled with the out-of-plane displacement component in the equations due to the non-homogeneity of an FGM. Asymptotic analysis of stress singularities in the vicinity of a sharp corner is carried out using the eigenfunction expansion approach. By assuming constant Poisson's ratio along the thickness, the characteristic equations for determining orders of stress singularity at the sharp corner are established for different sets of boundary conditions along the two radial edges forming the corner. The asymptotic solutions for the displacement functions are also explicitly presented. The effects of elasticity modulus variation along the thickness on stress singularity orders are thoroughly examined. These results are the first shown in the published literature.

2. Basic formulation

Consider a very thin wedge (or sector plate) (Fig. 1). The wedge is composed of FGM with material properties varying in the thickness direction (z-direction). That is, the wedge is non-homogeneous only in the thickness direction. The displacement field for the wedge with cylindrical coordinates (Fig. 1), based on the classical plate theory, is given as

$$\bar{u}(r,\theta,z) = u_0(r,\theta) - zw_{,r}, \tag{1a}$$

$$\bar{v}(r,\theta,z) = v_0(r,\theta) - \frac{z}{r}w_{,\theta}, \tag{1b}$$

$$\bar{w}(r,\theta,z) = w(r,\theta), \tag{1c}$$

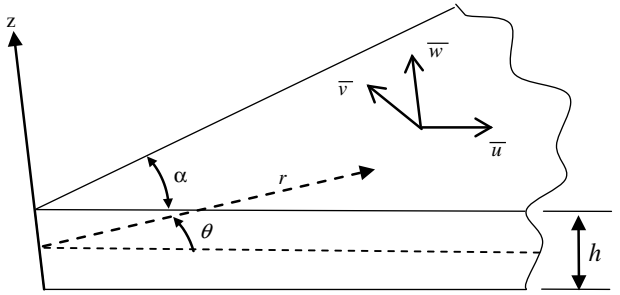

Fig. 1. Coordinate system and positive displacement components for a thin wedge.

where $\bar{u}$, $\bar{v}$, and $\bar{w}$ are the displacement components in r-, θ-, and z-directions, respectively; u_0, v_0, and w are the corresponding displacements on the mid-plane; the subscript "$,j$" denotes partial differentials with respect to the independent variable j; $-h/2 \leqslant z \leqslant h/2$, where h is the thickness of plate.

Introducing the following stress resultants:

$$(N_r, N_\theta, N_{r\theta}, Q_r, Q_\theta) = \int_{-h/2}^{h/2} (\sigma_{rr}, \sigma_{\theta\theta}, \sigma_{r\theta}, \sigma_{rz}, \sigma_{\theta z})\, \mathrm{d}z, \tag{2a}$$

$$(M_r, M_\theta, M_{r\theta}) = \int_{-h/2}^{h/2} z(\sigma_{rr}, \sigma_{\theta\theta}, \sigma_{r\theta})\, \mathrm{d}z, \tag{2b}$$

where σ_{ij} are stress components, and using the principle of stationary potential energy, one can obtain the equilibrium equations without external loading (cf. Reddy, 1999)

$$N_{r,r} + N_{r\theta,\theta}/r + (N_r - N_\theta)/r = 0, \tag{3a}$$

$$N_{r\theta,r} + N_{\theta,\theta}/r + 2N_{r\theta}/r = 0, \tag{3b}$$

$$Q_{r,r} + Q_{\theta,\theta}/r + Q_r/r = 0, \tag{3c}$$

$$M_{r,r} + M_{r\theta,\theta}/r + (M_r - M_\theta)/r - Q_r = 0, \tag{3d}$$

$$M_{r\theta,r} + M_{\theta,\theta}/r + 2M_{r\theta}/r - Q_\theta = 0. \tag{3e}$$

In addition, the following boundary conditions along $\theta = \alpha$ should be specified:

$$u_0 \text{ or } N_{r\theta}, \quad v_0 \text{ or } N_\theta, \quad w_{,\theta} \text{ or } M_\theta, \quad w \text{ or } V_\theta,$$

where effective shear force $V_\theta = Q_\theta + M_{r\theta,r}$. Along the r-constant edge, the following conditions should be prescribed:

$$u_0 \text{ or } N_r, \quad v_0 \text{ or } N_{r\theta}, \quad w_{,r} \text{ or } M_r, \quad w \text{ or } V_r,$$

where $V_r = Q_r + \frac{1}{r} M_{r\theta,\theta}$.

The displacement functions used in the classical theory (Eqs. (1)) result in zero transverse strain components (ε_{rz}, $\varepsilon_{\theta z}$ and ε_{zz}) and a plane strain case. Although $\varepsilon_{zz} = 0$ causes that the transverse normal stress σ_{zz} does not equal zero identically, σ_{zz} does not appear in the principle of stationary potential energy used to derive the equilibrium equations (Eqs. (3)). Consequently, the transverse stress is neglected, which implies a plane stress case. Nevertheless, a thin plate is in a state of plane stress from practical considerations because the thickness is very small compared to the in-plane dimension. The plane stress constitutive equations are applied in the following. Similar arguments are also given in Reddy's book (1999) for applying the classical plate theory to study the behaviors of laminated composite thin plates.

Using Eqs. (2), plane stress constitutive equations for an isotropic material and linear strain–displacement relations, the stress resultants can be expressed in terms of displacement functions as

$$N_r = \frac{\overline{D}_0}{r}u_0 + \overline{E}_0 u_{0,r} + \frac{\overline{D}_0}{r}v_{0,\theta} - \frac{\overline{D}_1}{r}w_{,r} - \overline{E}_1 w_{,rr} - \frac{\overline{D}_1}{r^2}w_{,\theta\theta}, \tag{4a}$$

$$N_\theta = \frac{\overline{E}_0}{r}u_0 + \overline{D}_0 u_{0,r} + \frac{\overline{E}_0}{r}v_{0,\theta} - \frac{\overline{E}_1}{r}w_{,r} - \overline{D}_1 w_{,rr} - \frac{\overline{E}_1}{r^2}w_{,\theta\theta}, \tag{4b}$$

$$N_{r\theta} = \frac{\overline{G}_0}{r}u_{0,\theta} - \frac{\overline{G}_0}{r}v_0 + \overline{G}_0 v_{0,r} + \frac{2\overline{G}_1}{r^2}w_{,\theta} - \frac{2\overline{G}_1}{r}w_{,r\theta}, \tag{4c}$$

$$M_r = \frac{\overline{D}_1}{r}u_0 + \overline{E}_1 u_{0,r} + \frac{\overline{D}_1}{r}v_{0,\theta} - \frac{\overline{D}_2}{r}w_{,r} - \overline{E}_2 w_{,rr} - \frac{\overline{D}_2}{r^2}w_{,\theta\theta}, \tag{4d}$$

$$M_\theta = \frac{\overline{E}_1}{r}u_0 + \overline{D}_1 u_{0,r} + \frac{\overline{E}_1}{r}v_{0,\theta} - \frac{\overline{E}_2}{r}w_{,r} - \overline{D}_2 w_{,rr} - \frac{\overline{E}_2}{r^2}w_{,\theta\theta}, \tag{4e}$$

$$M_{r\theta} = \frac{\overline{G}_1}{r}u_{0,\theta} - \frac{\overline{G}_1}{r}v_0 + \overline{G}_1 v_{0,r} + \frac{2\overline{G}_2}{r^2}w_{,\theta} - \frac{2\overline{G}_2}{r}w_{,r\theta}, \tag{4f}$$

where

$$\overline{G}_i = \int_{-h/2}^{h/2} G z^i \,\mathrm{d}z, \quad \overline{E}_i = \int_{-h/2}^{h/2} \frac{E}{1-\upsilon^2} z^i \,\mathrm{d}z, \quad \overline{D}_i = \int_{-h/2}^{h/2} \frac{\upsilon E}{1-\upsilon^2} z^i \,\mathrm{d}z \tag{5}$$

and G, E, and υ are shear modulus, modulus of elasticity, and Poisson's ratio, respectively, all of which can be functions of z. Since the displacement field given in Eqs. (1) leads to zero out-of-plane shear strains, the following relations between shear forces and displacement functions are obtained via equilibrium equations (Eqs. (3d, 3e)) and Eqs. (4d, 4e),

$$\begin{aligned} Q_r = {} & \frac{\overline{G}_1}{r^2}u_{0,\theta\theta} + \overline{E}_1\left(u_{0,rr} - \frac{u_0}{r^2} + \frac{u_{0,r}}{r}\right) + \frac{\overline{D}_1}{r}v_{0,r\theta} + \overline{G}_1\left(-\frac{v_{0,\theta}}{r^2} + \frac{v_{0,r\theta}}{r}\right) - \frac{\overline{E}_1}{r^2}v_{0,\theta} \\ & + \overline{G}_2\left(\frac{2w_{,\theta\theta}}{r^3} - \frac{2w_{,r\theta\theta}}{r^2}\right) + \overline{D}_2\left(\frac{w_{,\theta\theta}}{r^3} - \frac{w_{,r\theta\theta}}{r^2}\right) + \overline{E}_2\left(\frac{w_{,\theta\theta}}{r^3} + \frac{w_{,r}}{r^2} - \frac{w_{,rr}}{r} - w_{,rrr}\right), \end{aligned} \tag{6a}$$

$$\begin{aligned} Q_\theta = {} & \overline{G}_1\left(\frac{u_{0,\theta}}{r^2} + \frac{u_{0,r\theta}}{r}\right) + \frac{\overline{E}_1}{r^2}u_{0,\theta} + \frac{\overline{D}_1}{r}u_{0,r\theta} + \overline{G}_1\left(-\frac{v_0}{r^2} + \frac{v_{0,r}}{r} + v_{0,rr}\right) + \frac{\overline{E}_1}{r^2}v_{0,\theta\theta} \\ & - \frac{2\overline{G}_2}{r}w_{,rr\theta} - \overline{E}_2\left(\frac{w_{,\theta\theta\theta}}{r^3} + \frac{w_{,r\theta}}{r^2}\right) - \frac{\overline{D}_2}{r}w_{,rr\theta}. \end{aligned} \tag{6b}$$

Substituting Eqs. (4a)–(4c) and (6a), (6b) into Eqs. (3a)–(3c) yields the equilibrium equations for displacement functions as

$$\begin{aligned} & \overline{E}_0\left(-\frac{u_0}{r^2} + \frac{u_{0,r}}{r} + u_{0,rr} - \frac{v_{0,\theta}}{r^2}\right) + \overline{E}_1\left(\frac{w_{,r}}{r^2} - \frac{w_{,rr}}{r} - w_{,rrr} + \frac{w_{,\theta\theta}}{r^3}\right) + \overline{D}_0\left(\frac{v_{0,r\theta}}{r}\right) \\ & + \overline{D}_1\left(\frac{w_{,\theta\theta}}{r^3} - \frac{w_{,r\theta\theta}}{r^2}\right) + \overline{G}_0\left(-\frac{v_{0,\theta}}{r^2} + \frac{v_{0,r\theta}}{r} + \frac{u_{0,\theta\theta}}{r^2}\right) + \overline{G}_1\left(\frac{2w_{,\theta\theta}}{r^3} - \frac{2w_{,r\theta\theta}}{r^2}\right) = 0 \end{aligned} \tag{7a}$$

$$\begin{aligned} & \overline{E}_0\left(\frac{u_{0,\theta}}{r^2} + \frac{v_{0,\theta\theta}}{r^2}\right) + \overline{E}_1\left(-\frac{w_{,r\theta}}{r^2} - \frac{w_{,\theta\theta\theta}}{r^3}\right) + \overline{D}_0\left(\frac{u_{0,r\theta}}{r}\right) + \overline{D}_1\left(-\frac{w_{,rr\theta}}{r}\right) \\ & + \overline{G}_0\left(-\frac{v_0}{r^2} + \frac{v_{0,r}}{r} + v_{0,rr} + \frac{u_{0,\theta}}{r^2} + \frac{u_{0,r\theta}}{r}\right) + \overline{G}_1\left(-\frac{2w_{,rr\theta}}{r}\right) = 0 \end{aligned} \tag{7b}$$

$$\begin{aligned} & \overline{E}_1\left(\frac{u_0 + v_{0,\theta}}{r^3} - \frac{u_{0,r} + v_{0,r\theta}}{r^2} + \frac{2u_{0,rr}}{r} + u_{0,rrr} + \frac{u_{0,\theta\theta} + v_{0,\theta\theta\theta}}{r^3}\right) \\ & + \overline{E}_2\left(-\frac{w_{,r}}{r^3} + \frac{w_{,rr}}{r^2} - \frac{2w_{,\theta\theta}}{r^4} - \frac{2w_{,rrr}}{r} - \frac{w_{,\theta\theta\theta\theta}}{r^4} - w_{,rrrr}\right) + \overline{D}_1\left(\frac{v_{0,rr\theta}}{r} + \frac{u_{0,r\theta\theta}}{r^2}\right) \\ & + \overline{D}_2\left(-\frac{2w_{,\theta\theta}}{r^4} + \frac{2w_{,r\theta\theta}}{r^3} - \frac{2w_{,rr\theta\theta}}{r^2}\right) + \overline{G}_1\left(\frac{2v_{0,rr\theta}}{r} + \frac{2u_{0,r\theta\theta}}{r^2}\right) \\ & + \overline{G}_2\left(-\frac{4w_{,\theta\theta}}{r^4} + \frac{4w_{,r\theta\theta}}{r^3} - \frac{4w_{,rr\theta\theta}}{r^2}\right) = 0 \end{aligned} \tag{7c}$$

Each of Eqs. (7a)–(7c) involves u_0, v_0 and w. Accordingly, the in-plane displacement components on the mid-plane u_0 and v_0 are coupled with out-of-plane displacement w.

3. Asymptotic solutions

Using separation of variables, the homogenous solution of Eqs. (7) can be assumed as

$$u_0(r,\theta)=\Omega_u(r)U(\theta),\quad v_0(r,\theta)=\Omega_v(r)V(\theta),\quad \text{and}\quad w(r,\theta)=\Omega_w(r)W(\theta). \tag{8}$$

Based on the concept underlying the Frobenius method, the functions of r are expressed as a power series in r. Hence, Eq. (8) is further expressed as

$$u_0(r,\theta)=\sum_{n=0,1} r^{\lambda+n}U_n(\theta,\lambda),\quad v_0(r,\theta)=\sum_{n=0,1} r^{\lambda+n}V_n(\theta,\lambda),\quad \text{and}\quad w(r,\theta)=\sum_{n=0,1} r^{\lambda+n+1}W_n(\theta,\lambda), \tag{9}$$

where λ belongs to the set of complex numbers with positive real parts to meet the regularity requirement on displacement components at $r=0$. Substituting Eq. (9) into Eqs. (7) produces

$$\begin{aligned}
&\sum_n r^{\lambda+n-2}\{\overline{E}_0(\lambda+n-1)(\lambda+n+1)U_n+\overline{G}_0U_{n,\theta\theta}+((\lambda+n)\overline{D}_0-\overline{E}_0+(\lambda+n-1)\overline{G}_0)V_{n,\theta}\\
&\quad-\overline{E}_1(\lambda+n-1)(\lambda+n+1)^2W_n+(\overline{E}_1-(\lambda+n)(\overline{D}_1+2\overline{G}_1))W_{n,\theta\theta}\}=0, &\text{(10a)}\\
&\sum_n r^{\lambda+n-2}\{(\overline{E}_0+\overline{G}_0+(\lambda+n)(\overline{D}_0+\overline{G}_0))U_{n,\theta}+(\lambda+n-1)(\lambda+n+1)\overline{G}_0V_n\\
&\quad+\overline{E}_0V_{n,\theta\theta}-(\lambda+n+1)(\overline{E}_1+(\lambda+n)(\overline{D}_1+2\overline{G}_1))W_{n,\theta}-\overline{E}_1W_{n,\theta\theta\theta}\}=0, &\text{(10b)}\\
&\sum_n r^{\lambda+n-3}\{\overline{E}_1(\lambda+n-1)^2(\lambda+n+1)U_n+(\overline{E}_1+(\lambda+n)(\overline{D}_1+2\overline{G}_1))U_{n,\theta\theta}\\
&\quad+(\lambda+n-1)(-\overline{E}_1+(\lambda+n)(\overline{D}_1+2\overline{G}_1))V_{n,\theta}+\overline{E}_1V_{n,\theta\theta\theta}-\overline{E}_2(\lambda+n-1)^2(\lambda+n+1)^2W_n\\
&\quad+(-2\overline{E}_2-2(\lambda+n)^2(\overline{D}_2+2\overline{G}_2))W_{n,\theta\theta}-\overline{E}_2W_{n,\theta\theta\theta\theta}\}=0. &\text{(10c)}
\end{aligned}$$

To investigate the stress singularity features of solutions for Eqs. (10) in the neighborhood of $r=0$, only those solutions corresponding to the lowest order of r must be addressed. Consequently, the following equations corresponding to $n=0$ in Eqs. (10) must be solved:

$$\begin{aligned}
&\overline{E}_0(\lambda-1)(\lambda+1)U_0+\overline{G}_0U_{0,\theta\theta}+(\lambda\overline{D}_0-\overline{E}_0+(\lambda-1)\overline{G}_0)V_{0,\theta}\\
&\quad-\overline{E}_1(\lambda-1)(\lambda+1)^2W_0+(\overline{E}_1-\lambda(\overline{D}_1+2\overline{G}_1))W_{0,\theta\theta}=0, &\text{(11a)}\\
&(\overline{E}_0+\overline{G}_0+\lambda(\overline{D}_0+\overline{G}_0))U_{0,\theta}+(\lambda-1)(\lambda+1)\overline{G}_0V_0+\overline{E}_0V_{0,\theta\theta}\\
&\quad-(\lambda+1)(\overline{E}_1+\lambda(\overline{D}_1+2\overline{G}_1))W_{0,\theta}-\overline{E}_1W_{0,\theta\theta\theta}=0, &\text{(11b)}\\
&\overline{E}_1(\lambda-1)^2(\lambda+1)U_0+(\overline{E}_1+\lambda(\overline{D}_1+2\overline{G}_1))U_{0,\theta\theta}+(\lambda-1)(-\overline{E}_1+\lambda(\overline{D}_1+2\overline{G}_1))V_{0,\theta}+\overline{E}_1V_{0,\theta\theta\theta}\\
&\quad-\overline{E}_2(\lambda-1)^2(\lambda+1)^2W_0+(-2\overline{E}_2-2\lambda^2(\overline{D}_2+2\overline{G}_2))W_{0,\theta\theta}-\overline{E}_2W_{0,\theta\theta\theta\theta}=0. &\text{(11c)}
\end{aligned}$$

Eqs. (11) are a set of linear differential equations with constant coefficients. As the coefficients are not specified, obtaining an analytical solution in a simple explicit form is typically impossible. Hence, a further assumption regarding the material properties is made in the following. Since the variation range of Poisson's ratio is small and the stress singularity order at the interface corner in a bi-material isotropic plate is not sensitive to Poisson's ratio (Huang, 2002a), the Poisson's ratio is assumed constant through the thickness. Then, $\overline{D}_i$, $\overline{E}_i$, and $\overline{G}_i$ defined in Eq. (5) satisfy the following relations:

$$\overline{D}_i=\upsilon\overline{E}_i\quad\text{and}\quad\overline{G}_i=\frac{(1-\upsilon)}{2}\overline{E}_i. \tag{12}$$

Substituting Eq. (12) into Eqs. (11) and following a typical procedure for solving a set of linear differential equations, the general solutions for U_0, V_0, and W_0 are obtained as

$$U_0(\theta,\lambda) = A_1\cos(\lambda+1)\theta + A_2\sin(\lambda+1)\theta + A_3\cos(\lambda-1)\theta + A_4\sin(\lambda-1)\theta, \tag{13a}$$

$$V_0(\theta,\lambda) = A_2\cos(\lambda+1)\theta - A_1\sin(\lambda+1)\theta + (\kappa_1 A_4 - \kappa_2 B_4)\cos(\lambda-1)\theta + (-\kappa_1 A_3 + \kappa_2 B_3)\sin(\lambda-1)\theta, \tag{13b}$$

$$W_0(\theta,\lambda) = B_1\cos(\lambda+1)\theta + B_2\sin(\lambda+1)\theta + B_3\cos(\lambda-1)\theta + B_4\sin(\lambda-1)\theta, \tag{13c}$$

where $\kappa_1 = \frac{3+\lambda-\upsilon+\lambda\upsilon}{-3+\lambda+\upsilon+\lambda\upsilon}$ and $\kappa_2 = \frac{8\lambda}{(-3+\lambda+\upsilon+\lambda\upsilon)}\frac{\overline{E}_1}{\overline{E}_0}$. Coefficients A_i and B_i $(i=1,2,3,4)$ and λ are to be determined from boundary conditions along the radial edges. Notably, zero $\overline{E}_1$ yields the uncoupling between in-plane and out-of-plane displacement components on the mid-plane. In a brief summary, the solutions for Eqs. (7) with the assumption of constant Poisson's ratio along the thickness are

$$u_0(r,\theta) = r^{\lambda}\{A_1\cos(\lambda+1)\theta + A_2\sin(\lambda+1)\theta + A_3\cos(\lambda-1)\theta + A_4\sin(\lambda-1)\theta\} + O(r^{\lambda+1}), \tag{14a}$$

$$v_0(r,\theta) = r^{\lambda}\{A_2\cos(\lambda+1)\theta - A_1\sin(\lambda+1)\theta + (\kappa_1 A_4 - \kappa_2 B_4)\cos(\lambda-1)\theta + (-\kappa_1 A_3 + \kappa_2 B_3)\sin(\lambda-1)\theta\} + O(r^{\lambda+1}), \tag{14b}$$

$$w(r,\theta) = r^{\lambda+1}\{B_1\cos(\lambda+1)\theta + B_2\sin(\lambda+1)\theta + B_3\cos(\lambda-1)\theta + B_4\sin(\lambda-1)\theta\} + O(r^{\lambda+2}), \tag{14c}$$

where $O(r^{\lambda+1})$ are terms with order in r higher than (or equal to) $\lambda+1$. The relationship between displacement functions and stress resultants given in Eqs. (4) discloses that the singularities of the stress resultants (N_r, N_θ, $N_{r\theta}$, M_r, M_θ, and $M_{r\theta}$) exist when the real part of $\lambda < 1$.

4. Boundary conditions, characteristic equations and corner functions

After solving the equilibrium equations, attention is now turned to find out A_i, B_i and λ in the solutions from the boundary conditions along the radial edges forming a corner. A wedge with simply supported radial edges and a vertex angle α is utilized to demonstrate a typical procedure for deriving these coefficients and λ. The boundary conditions along a simply supported radial edge are $u_0 = v_0 = w = M_\theta = 0$, which simulate the mechanical support of a knife-edge along the mid-plane (see Fig. 2). By taking advantage of the problem's symmetry and considering $-\alpha/2 \leqslant \theta \leqslant \alpha/2$, the solutions given in Eqs. (14) are separated into symmetric and anti-symmetric parts. The symmetric solutions satisfying the boundary conditions yield

$$A_1\cos(\lambda+1)\frac{\alpha}{2} + A_3\cos(\lambda-1)\frac{\alpha}{2} = 0, \tag{15a}$$

$$-A_1\sin(\lambda+1)\frac{\alpha}{2} + [-\kappa_1 A_3 + \kappa_2 B_3]\sin(\lambda-1)\frac{\alpha}{2} = 0, \tag{15b}$$

$$B_1\cos(\lambda+1)\frac{\alpha}{2} + B_3\cos(\lambda-1)\frac{\alpha}{2} = 0, \tag{15c}$$

$$A_1(\upsilon-1)\lambda\overline{E}_1\cos(\lambda+1)\frac{\alpha}{2} - A_3(-1+(\lambda-1)\kappa_1 - \lambda\upsilon)\overline{E}_1\cos(\lambda-1)\frac{\alpha}{2} - B_1(\upsilon-1)\lambda(\lambda+1)\overline{E}_2\cos(\lambda+1)\frac{\alpha}{2} + B_3[\kappa_2(\lambda-1)\overline{E}_1 - \lambda(3+\lambda(\upsilon-1)+\upsilon)\overline{E}_2]\cos(\lambda-1)\frac{\alpha}{2} = 0. \tag{15d}$$

Eqs. (15) are a set of four linear algebraic equations for A_i and B_i ($i=1$ and 3). To have non-trivial solutions for A_i and B_i ($i=1$ and 3) yields a $4*4$ determinant equal to zero, which leads to:

$$\left(\cos(\lambda+1)\frac{\alpha}{2}\right)\left(\cos(\lambda-1)\frac{\alpha}{2}\right) = 0, \tag{16a}$$

or

$$\sin\lambda\alpha + \bar{\gamma}_1\sin\alpha = 0, \tag{16b}$$

where $\bar{\gamma}_1 = \frac{\lambda(-2\overline{E}_1^2+(1+\upsilon)\overline{E}_0\overline{E}_2)}{2\overline{E}_1^2+(-3+\upsilon)\overline{E}_0\overline{E}_2}$. Eqs. (16) are the characteristic equations of λ for symmetric solutions corresponding to the simply supported boundary conditions along two radial edges.

When λ satisfies $\sin\lambda\alpha + \bar{\gamma}_1\sin\alpha = 0$, the relations among A_i and B_i ($i=1$ and 3) are obtained from Eqs. (15). Then, the corresponding asymptotic solutions are

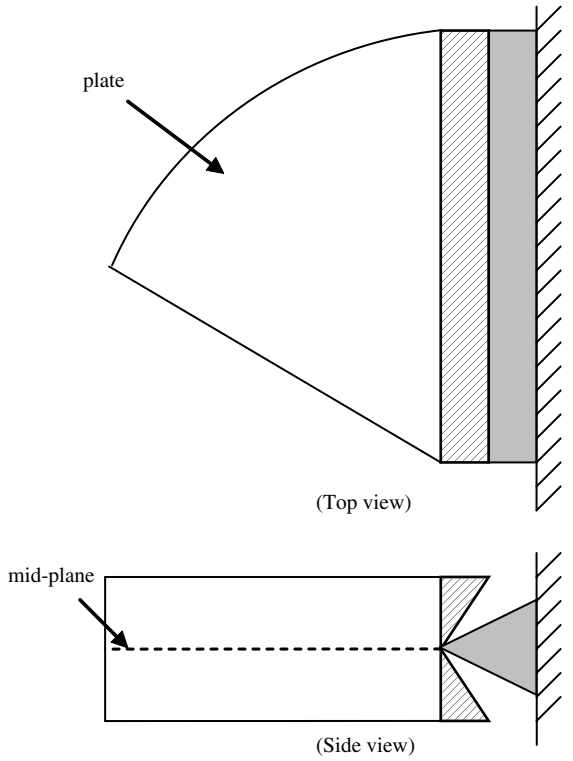

Fig. 2. Sketch of a plate having an edge with mechanical support of a knife-edge along the mid-plane.

$$u_0 = A_3 r^{\lambda}\left\{\left(-\frac{\cos(\lambda-1)\alpha/2}{\cos(\lambda+1)\alpha/2}\right)\cos(\lambda+1)\theta+\cos(\lambda-1)\theta\right\}, \tag{17a}$$

$$v_0 = A_3 r^{\lambda}\left\{\left(\frac{\cos(\lambda-1)\alpha/2}{\cos(\lambda+1)\alpha/2}\right)\sin(\lambda+1)\theta+(-\kappa_1+\kappa_2\bar{\eta}_1\sin(\lambda-1)\theta\right\}, \tag{17b}$$

$$w = A_3 r^{\lambda+1}\left\{\bar{\eta}_1\left[\left(-\frac{\cos(\lambda-1)\alpha/2}{\cos(\lambda+1)\alpha/2}\right)\cos(\lambda+1)\theta+\cos(\lambda-1)\theta\right]\right\}, \tag{17c}$$

where $\bar{\eta}_1 = \frac{1}{\kappa_2}\left(-\frac{\sin(\lambda+1)\alpha/2}{\sin(\lambda-1)\alpha/2}\frac{\cos(\lambda-1)\alpha/2}{\cos(\lambda+1)\alpha/2}+\kappa_1\right)$. These asymptotic solutions are also called corner functions corresponding to the characteristic equation $\sin\lambda\alpha+\bar{\gamma}_1\sin\alpha=0$. The asymptotic solutions for in-plane and out-of-plane displacement components on the mid-plane are coupled.

Similarly, one can find the corner functions corresponding to different characteristic equations (i.e., $\cos(\lambda-1)\frac{\alpha}{2}=0$ or $\cos(\lambda+1)\frac{\alpha}{2}=0$ in Eq. (16a)), which are listed in Table 1. Notably, the characteristic equation $\cos(\lambda-1)\frac{\alpha}{2}=0$ but $\cos(\lambda+1)\frac{\alpha}{2}\neq 0$ leads to $A_1=0$ and $B_3=\frac{\kappa_1}{\kappa_2}A_3$, and the solution of v_0 involving r^{λ} vanishes. The lowest order of r in the solution of v_0 will be $(\lambda+1)$, which can be observed from Eqs. (9) or (14b). This solution of v_0 does not produce stress singularities and is not given in Table 1. A similar situation also happens to the asymptotic solutions of u_0 and v_0 corresponding to $\cos(\lambda+1)\frac{\alpha}{2}=0$ but $\cos(\lambda-1)\frac{\alpha}{2}\neq 0$.

Using the anti-symmetric parts of solutions in Eqs. (14) and following the procedure above, the following characteristic equations are easily established:

$$(\sin(\lambda+1)\alpha/2)(\sin(\lambda-1)\alpha/2)=0, \tag{18a}$$

or

$$\sin\lambda\alpha-\bar{\gamma}_1\sin\alpha=0. \tag{18b}$$

The corner functions corresponding to these characteristic equations are also given in Table 1. The characteristic equation $(\sin(\lambda+1)\alpha/2)(\sin(\lambda-1)\alpha/2)=0$ may also result in the asymptotic solutions of u_0 or v_0 with the

Table 1
Corner functions corresponding to different boundary conditions

Boundary conditions	Corner functions
Simply supported–simply supported (S–S) $(-\alpha/2 \leqslant \theta \leqslant \alpha/2)$	(1) Symmetric case When $(\cos(\lambda-1)\alpha/2)=0$ and $\cos(\lambda+1)\alpha/2)\neq 0$, $u_0 = A_3 r^{\lambda}\{cos(\lambda-1)\theta\}$, $w = A_3 r^{\lambda+1}\left\{\frac{\kappa_1}{\kappa_2}\cos(\lambda-1)\theta\right\}$. When $(\cos(\lambda+1)\alpha/2)=0$ and $(\cos(\lambda-1)\alpha/2)\neq 0$, $w = B_1 r^{\lambda+1}\{\cos(\lambda+1)\theta\}$. When $(\cos(\lambda-1)\alpha/2)=0$ and $(\cos(\lambda+1)\alpha/2)=0$, $u_0 = r^{\lambda}\left\{A_3\left[\left(-\frac{\sin(\lambda-1)\alpha/2}{\sin(\lambda+1)\alpha/2}\right)\kappa_1\cos(\lambda+1)\theta+\cos(\lambda-1)\theta\right]\right.$ $\left.+B_3\left[\left(\frac{\sin(\lambda-1)\alpha/2}{\sin(\lambda+1)\alpha/2}\right)\kappa_2\cos(\lambda+1)\theta\right]\right\}$, $v_0 = r^{\lambda}\left\{(-\kappa_1 A_3+\kappa_2 B_3)\left[\left(-\frac{\sin(\lambda-1)\alpha/2}{\sin(\lambda+1)\alpha/2}\right)\sin(\lambda+1)\theta+\sin(\lambda-1)\theta\right]\right\}$, $w = r^{\lambda+1}\{B_1\cos(\lambda+1)\theta+B_3\cos(\lambda-1)\theta\}$. When $\bar{\gamma}_1\sin\alpha+\sin\lambda\alpha=0$, $u_0 = A_3 r^{\lambda}\left\{\left(-\frac{\cos(\lambda-1)\alpha/2}{\cos(\lambda+1)\alpha/2}\right)\cos(\lambda+1)\theta+\cos(\lambda-1)\theta\right\}$, $v_0 = A_3 r^{\lambda}\left\{\left(\frac{\cos(\lambda-1)\alpha/2}{\cos(\lambda+1)\alpha/2}\right)\sin(\lambda+1)\theta+(-\kappa_1+\kappa_2\bar{\eta}_1)\sin(\lambda-1)\theta\right\}$, $w = A_3 r^{\lambda+1}\left\{\bar{\eta}_1\left[\left(-\frac{\cos(\lambda-1)\alpha/2}{\cos(\lambda+1)\alpha/2}\right)\cos(\lambda+1)\theta+\cos(\lambda-1)\theta\right]\right\}$, where $\bar{\eta}_1 = \frac{1}{\kappa_2}\left[\left(\frac{\sin(\lambda+1)\alpha/2}{\sin(\lambda-1)\alpha/2}\right)\left(-\frac{\cos(\lambda-1)\alpha/2}{\cos(\lambda+1)\alpha/2}\right)+\kappa_1\right]$.
Simply supported–simply supported (S–S) $(-\alpha/2 \leqslant \theta \leqslant \alpha/2)$	(2) Anti-symmetric case When $(\sin(\lambda-1)\alpha/2)=0$ and $(\sin(\lambda+1)\alpha/2)\neq 0$, $u_0 = A_4 r^{\lambda}\{\sin(\lambda-1)\theta\}$, $w = A_4 r^{\lambda+1}\left\{\frac{\kappa_1}{\kappa_2}\sin(\lambda-1)\theta\right\}$. When $(\sin(\lambda+1)\alpha/2)=0$ and $(\sin(\lambda-1)\alpha/2)\neq 0$, $w = B_2 r^{\lambda+1}\{\sin(\lambda+1)\theta\}$. When $(\sin(\lambda-1)\alpha/2)=0$ and $(\sin(\lambda+1)\alpha/2)=0$, $u_0 = r^{\lambda}\left\{A_4\left[-\left(\frac{\cos(\lambda-1)\alpha/2}{\cos(\lambda+1)\alpha/2}\right)\kappa_1\sin(\lambda+1)\theta+\sin(\lambda-1)\theta\right]\right.$ $\left.+B_4\left[\left(\frac{\cos(\lambda-1)\alpha/2}{\cos(\lambda+1)\alpha/2}\right)\kappa_2\sin(\lambda+1)\theta\right]\right\}$, $v_0 = r^{\lambda}\left\{(\kappa_1 A_4-\kappa_2 B_4)\left[-\left(\frac{\cos(\lambda-1)\alpha/2}{\cos(\lambda+1)\alpha/2}\right)\cos(\lambda+1)\theta+\cos(\lambda-1)\theta\right]\right\}$, $w = r^{\lambda+1}\{B_2\sin(\lambda+1)\theta+B_4 sin(\lambda-1)\theta\}$. When $\sin\lambda\alpha-\bar{\gamma}_1\sin\alpha=0$, $u_0 = A_4 r^{\lambda}\left\{\left(-\frac{\sin(\lambda-1)\alpha/2}{\sin(\lambda+1)\alpha/2}\right)\sin(\lambda+1)\theta+\sin(\lambda-1)\theta\right\}$, $v_0 = A_4 r^{\lambda}\left\{\left(-\frac{\sin(\lambda-1)\alpha/2}{\sin(\lambda+1)\alpha/2}\right)\cos(\lambda+1)\theta+(\kappa_1-\kappa_2\bar{\eta}_2)\cos(\lambda-1)\theta\right\}$, $w = A_4 r^{\lambda+1}\left\{\bar{\eta}_2\left[\left(-\frac{\sin(\lambda-1)\alpha/2}{\sin(\lambda+1)\alpha/2}\right)\sin(\lambda+1)\theta+\sin(\lambda-1)\theta\right]\right\}$, where $\bar{\eta}_2 = \frac{1}{\kappa_2}\left[\left(-\frac{\sin(\lambda-1)\alpha/2}{\sin(\lambda+1)\alpha/2}\right)\left(\frac{\cos(\lambda+1)\alpha/2}{\cos(\lambda-1)\alpha/2}\right)+\kappa_1\right]$.

(*continued on next page*)

Table 1 (*continued*)

Boundary conditions	Corner functions
Free–free (F–F) ($-\alpha/2 \leqslant \theta \leqslant \alpha/2$)	(1) Symmetric case $u_0 = B_3 r^{\lambda}\left\{\bar{\eta}_3\left(\frac{\cos(\lambda-1)\alpha/2}{\cos(\lambda+1)\alpha/2}\right)\cos(\lambda+1)\theta + \bar{\eta}_4\cos(\lambda-1)\theta\right\}$, $v_0 = B_3 r^{\lambda}\left\{-\bar{\eta}_3\left(\frac{\cos(\lambda-1)\alpha/2}{\cos(\lambda+1)\alpha/2}\right)\sin(\lambda+1)\theta + (-\kappa_1\bar{\eta}_4+\kappa_2)\sin(\lambda-1)\theta\right\}$, $w = B_3 r^{\lambda+1}\left\{\bar{\eta}_5\left(\frac{\cos(\lambda-1)\alpha/2}{\cos(\lambda+1)\alpha/2}\right)\cos(\lambda+1)\theta + \cos(\lambda-1)\theta\right\}$, where $\bar{\eta}_3 = -\frac{[3+\lambda(-1+\upsilon)+\upsilon]\overline{E}_1}{(-1+\upsilon)\overline{E}_0}$, $\bar{\eta}_4 = \frac{(\lambda+1)\overline{E}_1}{\overline{E}_0}$, $\bar{\eta}_5 = -\frac{[3+\lambda(-1+\upsilon)+\upsilon]}{(\lambda+1)(-1+\upsilon)}$. (2) Anti-symmetric case $u_0 = B_4 r^{\lambda}\left\{\bar{\eta}_3\left(\frac{\sin(\lambda-1)\alpha/2}{\sin(\lambda+1)\alpha/2}\right)\sin(\lambda+1)\theta + \bar{\eta}_4\sin(\lambda-1)\theta\right\}$, $v_0 = B_4 r^{\lambda}\left\{\bar{\eta}_3\left(\frac{\sin(\lambda-1)\alpha/2}{\sin(\lambda+1)\alpha/2}\right)\cos(\lambda+1)\theta + (\kappa_1\bar{\eta}_4-\kappa_2)\cos(\lambda-1)\theta\right\}$, $w = B_4 r^{\lambda+1}\left\{\bar{\eta}_5\left(\frac{\sin(\lambda-1)\alpha/2}{\sin(\lambda+1)\alpha/2}\right)\sin(\lambda+1)\theta + \sin(\lambda-1)\theta\right\}$.
Clamped–clamped (C–C) ($-\alpha/2 \leqslant \theta \leqslant \alpha/2$)	(1) Symmetric case $u_0 = A_3 r^{\lambda}\left\{\left(-\frac{\cos(\lambda-1)\alpha/2}{\cos(\lambda+1)\alpha/2}\right)\cos(\lambda+1)\theta + \cos(\lambda-1)\theta\right\}$, $v_0 = A_3 r^{\lambda}\left\{\left(\frac{\cos(\lambda-1)\alpha/2}{\cos(\lambda+1)\alpha/2}\right)\sin(\lambda+1)\theta + (-\kappa_1+\kappa_2\bar{\eta}_1)\sin(\lambda-1)\theta\right\}$, $w = A_3 r^{\lambda+1}\left\{\bar{\eta}_1\left[\left(-\frac{\cos(\lambda-1)\alpha/2}{\cos(\lambda+1)\alpha/2}\right)\cos(\lambda+1)\theta + \cos(\lambda-1)\theta\right]\right\}$. (2) Anti-symmetric case $u_0 = A_4 r^{\lambda}\left\{\left(-\frac{\sin(\lambda-1)\alpha/2}{\sin(\lambda+1)\alpha/2}\right)\sin(\lambda+1)\theta + \sin(\lambda-1)\theta\right\}$, $v_0 = A_4 r^{\lambda}\left\{\left(-\frac{\sin(\lambda-1)\alpha/2}{\sin(\lambda+1)\alpha/2}\right)\cos(\lambda+1)\theta + (\kappa_1-\kappa_2\bar{\eta}_2)\cos(\lambda-1)\theta\right\}$, $w = A_4 r^{\lambda+1}\left\{\bar{\eta}_2\left[\left(-\frac{\sin(\lambda-1)\alpha/2}{\sin(\lambda+1)\alpha/2}\right)\sin(\lambda+1)\theta + \sin(\lambda-1)\theta\right]\right\}$.
Free–clamped (F–C) ($0 \leqslant \theta \leqslant \alpha$)	$u_0 = B_3 r^{\lambda}\{[\bar{\eta}_3\cos(\lambda+1)\theta + \bar{\eta}_6\frac{\overline{E}_1}{\overline{E}_0}\sin(\lambda+1)\theta + \bar{\eta}_4\cos(\lambda-1)\theta + \bar{\eta}_7\frac{\overline{E}_1}{\overline{E}_0}\sin(\lambda-1)\theta]\}$, $v_0 = B_3 r^{\lambda}\{[\bar{\eta}_6\frac{\overline{E}_1}{\overline{E}_0}\cos(\lambda+1)\theta - \bar{\eta}_3\sin(\lambda+1)\theta + (\kappa_1\bar{\eta}_7\frac{\overline{E}_1}{\overline{E}_0}(\lambda+1) - \kappa_2\bar{\eta}_7)\cos(\lambda-1)\theta + (-\kappa_1\bar{\eta}_4+\kappa_2)\sin(\lambda-1)\theta]\}$, $w = B_3 r^{\lambda+1}\left\{\left[\bar{\eta}_5\cos(\lambda+1)\theta + \frac{\bar{\eta}_6}{(\lambda+1)}\sin(\lambda+1)\theta + \cos(\lambda-1)\theta + \bar{\eta}_7\sin(\lambda-1)\theta\right]\right\}$, where $\bar{\eta}_6 = \frac{-(\lambda^2-1)(\upsilon-1)+\lambda(3+\lambda(\upsilon-1)+\upsilon)\cos 2\alpha - (3+\lambda(\upsilon-1)+\upsilon)\cos 2\lambda\alpha}{(\upsilon-1)(\lambda\sin 2\alpha - \sin 2\lambda\alpha)}$, $\bar{\eta}_7 = \frac{-3+\lambda-\upsilon-\lambda\upsilon+\lambda(\upsilon-1)\cos 2\alpha + (\upsilon-1)\cos 2\lambda\alpha}{(\upsilon-1)(\lambda\sin 2\alpha - \sin 2\lambda\alpha)}$.

Table 1 (*continued*)

Boundary conditions	Corner functions
Simply supported–clamped (S–C) ($0 \leqslant \theta \leqslant \alpha$)	$u_0 = B_3 r^{\lambda}\{\bar{\eta}_{10}(-2\sin\theta\sin\lambda\theta) - \bar{\eta}_{11}\sin(\lambda+1)\theta + \bar{\eta}_{12}\sin(\lambda-1)\theta\}$, $v_0 = B_3 r^{\lambda}\{[-\bar{\eta}_{11}\cos(\lambda+1)\theta - \bar{\eta}_{10}\sin(\lambda+1)\theta$ $+ (\kappa_1\bar{\eta}_{12} - \kappa_2\bar{\eta}_9)\cos(\lambda-1)\theta + (\kappa_1\bar{\eta}_{10} + \kappa_2)\sin(\lambda-1)\theta]\}$, $w = B_3 r^{\lambda+1}\{[-\cos(\lambda+1)\theta + \bar{\eta}_8\sin(\lambda+1)\theta + \cos(\lambda-1)\theta + \bar{\eta}_9\sin(\lambda-1)\theta]\}$, where $\bar{\eta}_8 = -\dfrac{-1+\lambda-\lambda\cos 2\alpha+\cos 2\lambda\alpha}{\lambda\sin 2\alpha - \sin 2\lambda\alpha}$, $\bar{\eta}_9 = -\dfrac{-1-\lambda+\lambda\cos 2\alpha+\cos 2\lambda\alpha}{\lambda\sin 2\alpha - \sin 2\lambda\alpha}$, $\bar{\eta}_{10} = \dfrac{\kappa_2(1-\lambda)\overline{E}_1 + 4\lambda\overline{E}_2}{[-1+\kappa_1(\lambda-1)-\lambda]\overline{E}_1}$, $\bar{\eta}_{11} = \dfrac{-2\kappa_1\bar{\eta}_{10}\sin\alpha\sin\lambda\alpha + \kappa_2\bar{\eta}_9\sin(\lambda-1)\alpha}{\kappa_1\sin(\lambda+1)\alpha - \sin(\lambda-1)\alpha}$, $\bar{\eta}_{12} = \{(\lambda-1)\lambda\sin(\lambda-3)\alpha + \lambda(\kappa_1+2\lambda-\kappa_1\lambda)\sin(\lambda+3)\alpha$ $- \kappa_1(\lambda-1)^2\sin(\lambda-1)\alpha + [-3-\lambda(2+3\lambda)+2\kappa_1(\lambda_2-1)]\sin(\lambda+1)\alpha$ $+ (2+\kappa_1-\kappa_1\lambda)\sin(3\lambda+1)\alpha + (\lambda-1)\sin(3\lambda-1)\alpha\}/\{2\overline{E}_1(-1+\kappa_1(\lambda-1)-\lambda)$ $(-\lambda\sin 2\alpha + \sin 2\lambda\alpha)[\sin(\lambda-1)\alpha - \kappa_1\sin(\lambda+1)\alpha]\}$.
Free–simply supported (F–S) ($0 \leqslant \theta \leqslant \alpha$)	$u_0 = B_3 r^{\lambda}\{[\bar{\eta}_{18}\cos(\lambda+1)\theta + \bar{\eta}_{16}\sin(\lambda+1)\theta + \bar{\eta}_{19}\cos(\lambda-1)\theta + \bar{\eta}_{17}\sin(\lambda-1)\theta]/\bar{\eta}_{14}\}$, $v_0 = B_3 r^{\lambda}\{[(\bar{\eta}_{16}/\bar{\eta}_{14})\cos(\lambda+1)\theta - (\bar{\eta}_{18}/\bar{\eta}_{14})\sin(\lambda+1)\theta$ $+ [\kappa_1(\bar{\eta}_{17}/\bar{\eta}_{14}) - \kappa_2\bar{\eta}_{15}]\cos(\lambda-1)\theta + [-\kappa_1(\bar{\eta}_{19}/\bar{\eta}_{14}) + \kappa_2]\sin(\lambda-1)\theta]\}$, $w = B_3 r^{\lambda+1}\{[\bar{\eta}_5\cos(\lambda+1)\theta - \bar{\eta}_{13}\bar{\eta}_{15}\sin(\lambda+1)\theta + \cos(\lambda-1)\theta + \bar{\eta}_{15}\sin(\lambda-1)\theta]\}$, where $\bar{\eta}_{13} = \dfrac{(-3+\lambda(\upsilon-1)-\upsilon)}{(\upsilon-1)(\lambda+1)}$, $\bar{\eta}_{14} = \overline{E}_0(\upsilon-1)[5+(\upsilon-2)\upsilon - \lambda^2(\upsilon+1)^2 + \lambda^2(\upsilon+1)^2\cos 2\alpha$ $- (\upsilon-3)(\upsilon+1)\cos\lambda\alpha][-(-2+\lambda(\upsilon-1))\cos\lambda\alpha\sin\alpha + (\upsilon+1)\cos\alpha\sin\lambda\alpha]$, $\bar{\eta}_{15} = \dfrac{-2\cos\alpha\cos\lambda\alpha + (1+\lambda(\upsilon-1)+\upsilon)\sin\alpha + \sin\lambda\alpha}{(-2+\lambda(\upsilon-1))\cos\lambda\alpha\sin\alpha - (\upsilon+1)\cos\alpha\sin\lambda\alpha}$, $\bar{\eta}_{16} = -2\overline{E}_1\{\lambda^2(\lambda+\upsilon)(\upsilon^2-1)\cos(\lambda-3)\alpha - [3+10\lambda+\lambda^2-2\lambda^3-4(\lambda^2+1)\upsilon$ $+ (1+\lambda(6+\lambda(3+2\lambda)))\upsilon^2]\cos(\lambda-1)\alpha - [-10-3\lambda+2\lambda^2-\lambda^3$ $+ (2+\lambda(3+\lambda(6+\lambda)))\upsilon^2]\cos(\lambda+1)\alpha - \lambda^2(\upsilon+1)^3\cos(\lambda+3)\alpha$ $- \lambda(-3+\lambda\upsilon)(\upsilon^2-1)\cos(1-3\lambda)\alpha$ $+ (\upsilon+1)[-3+(-1+\lambda^2(\upsilon-1))\upsilon]\cos(1+3\lambda)\alpha\}$, $\bar{\eta}_{17} = -2\overline{E}_1\{\lambda^2(\upsilon-1)^2(-1+\lambda+\upsilon+\lambda\upsilon)\cos(\lambda-3)\alpha + [-2(\lambda+1)(\lambda^2-5)$ $+ \lambda\upsilon(\lambda-3)(3\lambda-1) + 2(\lambda+1)^3\upsilon^2 - 3\lambda(\lambda+1)^2\upsilon^3]\cos(\lambda-1)\alpha$ $+ [-3+\lambda(3+\lambda(\lambda-1)) - 4\upsilon - 3(\lambda-1)^2\lambda\upsilon - (\lambda+1)^3\upsilon^2$ $+ 3\lambda(\lambda+1)^2\upsilon^3]\cos(\lambda+1)\alpha - \lambda^2(\lambda+1)\upsilon(\upsilon^2-1)\cos(\lambda+3)\alpha$ $- (\upsilon-1)[3-\upsilon+\lambda(\upsilon-1)(-3+\upsilon+\lambda\upsilon)]\cos(1-3\lambda)\alpha$ $+ \lambda(\lambda+1)\upsilon(\upsilon^2-1)\cos(1+3\lambda)\alpha\}$, $\bar{\eta}_{18} = 2\overline{E}_1\{\lambda^2(\lambda+1)\upsilon(\upsilon^2-1)\sin(\lambda-3)\alpha + \lambda^2(\upsilon+1)^3\sin(\lambda+3)\alpha$ $- (\upsilon-1)[-3+\upsilon+\lambda(\lambda+(2+\lambda(2\lambda-1))\upsilon + 2(\lambda^2+\lambda+1)\upsilon^2)]\sin(\lambda-1)\alpha$ $+ [-2(-5+\upsilon^2) + \lambda^3\upsilon(\upsilon^2-1) - 2\lambda^2(1+3\upsilon^2) + \lambda\upsilon(1-\upsilon^2)]\sin(\lambda+1)\alpha$ $+ [3+\upsilon(4+\upsilon-\lambda^2(\upsilon^2-1))]\sin(1+3\lambda)\alpha$ $+ \lambda(\lambda+1)\upsilon(\upsilon^2-1)\sin(-1+3\lambda)\alpha\}$, $\bar{\eta}_{19} = 2\overline{E}_1\{-\lambda^2(\upsilon-1)^2(-1+\lambda+\upsilon+\lambda\upsilon)\sin(\lambda-3)\alpha$ $- \lambda^2(\lambda+\upsilon)(\upsilon^2-1)\sin(\lambda+3)\alpha$ $+ [10+\lambda(-13+\lambda(-2+3\lambda)) - 2\lambda\upsilon(1+(\lambda-7)\lambda) - (2+3\lambda(\lambda+1)^2)\upsilon^2$ $+ 2\lambda(\lambda^2+\lambda+1)\upsilon^3]\sin(\lambda-1)\alpha + [-\lambda^3(\upsilon-3)(\upsilon-1)(\upsilon+1)$.

Table 2
Characteristic equations

Boundary conditions	Characteristic equations
S–S	Symmetry : $(\cos(\lambda+1)\alpha/2)(\cos(\lambda-1)\alpha/2)=0^{*}$; $\bar{\gamma}_1\sin\alpha+\sin\lambda\alpha=0$; where $\bar{\gamma}_1=\frac{\bar{\kappa}_1}{\bar{\kappa}_2}$, $\bar{\kappa}_1=\lambda[-2\overline{E}_1^2+(1+\upsilon)\overline{E}_0\overline{E}_2]$, $\bar{\kappa}_2=2\overline{E}_1^2+(-3+\upsilon)\overline{E}_0\overline{E}_2$ Anti-symmetry : $(\sin(\lambda+1)\alpha/2)(\sin(\lambda-1)\alpha/2)=0^{*}$; $\sin\lambda\alpha-\bar{\gamma}_1\sin\alpha=0$.
F–F	Symmetry : $[\lambda(-1+\upsilon)\sin\alpha+(3+\upsilon)\sin\lambda\alpha]=0^{*}$; $(\lambda\sin\alpha+\sin\lambda\alpha)=0^{\#}$ Anti-symmetry : $[-\lambda(-1+\upsilon)\sin\alpha+(3+\upsilon)\sin\lambda\alpha]=0^{*}$; $(-\lambda\sin\alpha+\sin\lambda\alpha)=0^{\#}$
C–C	Symmetry : $(\lambda\sin\alpha+\sin\lambda\alpha)=0^{*}$; $[\lambda(1+\upsilon)\sin\alpha+(-3+\upsilon)\sin\lambda\alpha]=0^{\#}$ Anti-symmetry : $(-\lambda\sin\alpha+\sin\lambda\alpha)=0^{*}$; $[\lambda(1+\upsilon)\sin\alpha-(-3+\upsilon)\sin\lambda\alpha]=0^{\#}$
F–C	$4-\lambda^2(-1+\upsilon)^2\sin^2\alpha+(3+\upsilon)(-1+\upsilon)\sin^2\lambda\alpha=0^{*}$ $-4+\lambda^2(1+\upsilon)^2\sin^2\alpha-(-3+\upsilon)(1+\upsilon)\sin^2\lambda\alpha=0^{\#}$
S–C	$-\overline{E}_0\overline{E}_2[\lambda^2(1+\upsilon)^2 sin^2\alpha-(-3+\upsilon)^2\sin^2\lambda\alpha](-\lambda\sin2\alpha+\sin2\lambda\alpha)$ $+2\overline{E}_1^2\{-\lambda^2\sin^2\alpha[\lambda(1+\upsilon)\sin2\alpha+(1-3\upsilon)\sin2\lambda\alpha]+$ $+\sin^2\lambda\alpha[-\lambda(-5+3\upsilon)\sin2\alpha+(-3+\upsilon)\sin2\lambda\alpha]\}=0$
F–S	$-\overline{E}_0\overline{E}_2[-4+\lambda^2(1+\upsilon)^2\sin^2\alpha-(-3+\upsilon)(1+\upsilon)\sin^2\lambda\alpha]$ $\times(-\lambda(-1+\upsilon)\sin2\alpha+(3+\upsilon)\sin2\lambda\alpha)$ $+2\overline{E}_1^2\{-\lambda\sin2\alpha[4+\lambda^2(-1+\upsilon^2)\sin^2\alpha+3(-1+\upsilon^2)\sin^2\lambda\alpha]$ $+\sin2\lambda\alpha[-4+\lambda^2(1+\upsilon)(1+3\upsilon)\sin^2\alpha+(1+\upsilon)(1+3\upsilon)\sin^2\lambda\alpha]\}=0$

Note:
* Means that the equation is identical to that for a homogeneous plate under bending.
# Means that the equation is identical to that for a homogeneous plate under extension.
S, C and F denote simply supported, clamped and free boundary conditions, respectively.

order of r larger than λ, which are not shown in Table 1, similar to what happens to the asymptotic solutions corresponding to $\cos(\lambda+1)\frac{\alpha}{2}=0$ or $\cos(\lambda-1)\frac{\alpha}{2}=0$ shown above.

Characteristic equations (16a) and (18a) do not involve material properties, and are identical to the characteristic equations for a homogeneous thin wedge with two simply supported radial edges under bending. However, material properties are involved in the characteristic equations (16b) and (18b).

The characteristic equations for all combinations of fixed, free and simply supported boundary conditions have been obtained and summarized in Table 2, while the corresponding corner functions are all listed in Table 1. Notably, the results in these tables were obtained by taking advantage of the symmetry of the problem and considering $-\alpha/2\leqslant\theta\leqslant\alpha/2$ when the same boundary conditions are imposed along the two radial edges. These results are the first shown in the published literature.

Table 2 reveals that the characteristic equations corresponding to the boundary conditions without involving simply supported conditions are identical to the combination of the characteristic equations for homogeneous plates under bending and extension. The non-homogeneity considered here does not influence the stress

singularity orders at the corner of a thin plate if one of the two radial edges around the corner is not simply supported. However, Table 1 shows that most of the asymptotic solutions for the in-plane and out-of-plane displacement components on the mid-plane are coupled and are significantly different from those for homogenous plates.

5. Numerical results for λ

To demonstrate the effects of material non-homogeneity on stress singularity orders, a typical non-homogeneity is considered, assuming the variations of the Young's modulus through the thickness of plate given as

$$E(z) = E_b + V(z)\Delta E, \tag{19}$$

where $V(z) = (z/h + 1/2)^m$, E_b is the value of Young's modulus at $z = -h/2$ and ΔE is the difference between the values of Young's modulus at $z = h/2$ and $z = -h/2$. Consequently,

$$\overline{E}_0 = E_b h\left[\frac{1}{1-\upsilon^2} + \frac{\Delta E/E_b}{(1+m)(1-\upsilon^2)}\right], \tag{20a}$$

$$\overline{E}_1 = E_b h^2\left[\frac{m(\Delta E/E_b)}{2(1+m)(2+m)(1-\upsilon^2)}\right], \tag{20b}$$

$$\overline{E}_2 = E_b h^3\left[\frac{1}{12(1-\upsilon^2)} + \frac{(2+m+m^3)(\Delta E/E_b)}{4(1+m)(2+m)(3+m)(1-\upsilon^2)}\right]. \tag{20c}$$

The roots of the characteristic equations corresponding to boundary conditions involving simple support (see Table 2) depend on m, υ and $\Delta E/E_b$. The Poisson's ratio is set equal to 0.3 for the results shown below. The roots of the characteristic equations considered below, except for Eqs. (16a) and (18a), were accurately obtained by the numerical technique proposed by Müller (1956). The roots of Eqs. (16a) and (18a) were analytically determined.

Fig. 3 depicts the variation of the minimum real parts of λ (Re[λ]) with the material properties and the vertex angle of a wedge having simply-supported radial edges. The roots of Eqs. (16a), (16b), (18a), and (18b) were obtained independently. An infinite number of roots exist for each of these equations. Only the root with a minimum real part is important as it determines the stress singularity order at the vertex. The minimum values of Re[λ] obtained from Eq. (16a), independent of material properties, are smaller than those for Eq. (16b) for a wide range of material properties. Similarly, minimum values of Re[λ] determined from Eq. (18a) are less than those for Eq. (18b) with different material properties when minimum Re[λ] is less than unity. As a result, the singularity order of the stress resultants at a sharp corner with simply-supported edges is very likely determined by Eq. (16a) or (18a), independent of material properties.

Figs. 4–6 illustrate the effects of material non-homogeneity on the minimum Re[λ] of the characteristic equation corresponding to simply supported-clamped boundary condition. When $m = 0$ or $\Delta E = 0$, which generates homogeneous thin plates, the characteristic equation for simply supported-clamped boundary condition given in Table 2 yields

$$\lambda^2(1+\upsilon)^2\sin^2\alpha - (-3+\upsilon)^2\sin^2\lambda\alpha = 0, \tag{21a}$$

$$\text{or} \quad -\lambda\sin 2\alpha + \sin 2\lambda\alpha = 0. \tag{21b}$$

Eq. (21a) is identical to the characteristic equation obtained by Williams (1952a) for a homogeneous wedge with fixed radial edges under extension, whereas Eq. (21b) is the same as that given by Williams (1952b) for a homogeneous wedge with simply supported and clamped radial edges under bending.

Fig. 4 shows that the minimum Re[λ] of Eq. (21b) is smaller than that of Eq. (21a), indicating that bending produces more severe stress singularities than does extension at the vertex of a homogeneous wedge. Material non-homogeneity causes the minimum Re[λ] of the characteristic equation to be somewhat different from that of Eq. (21b). The stress singularities at the vertex are not present when the vertex angle is less than roughly 120°.

In order to further investigate the effects of material non-homogeneity on stress singularities, Fig. 5 displays the effects of m on the minimum Re[λ], where $\Delta E/E_b = 10$; and Fig. 6 shows the effects of $\Delta E/E_b$ on the min-

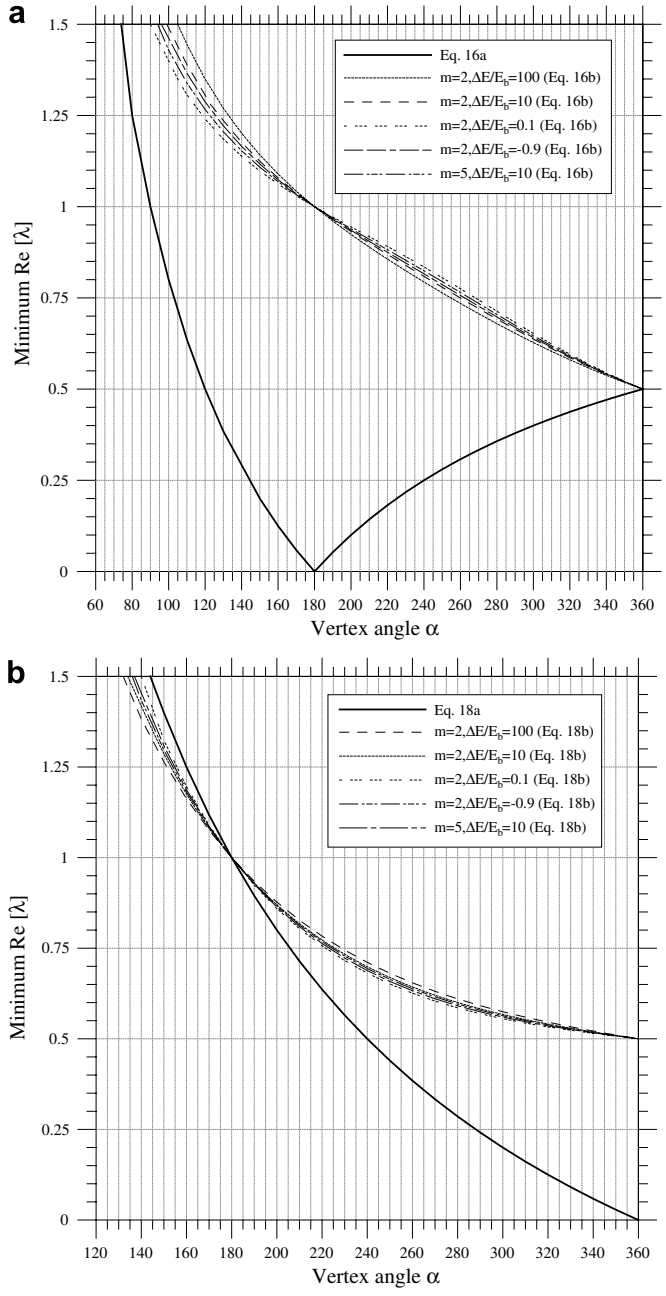

Fig. 3. Minimum Re[λ] of characteristic equations corresponding to simply supported–simply supported boundary condition: (a) symmetric solution, (b) anti-symmetric solution.

imum Re[λ], where $m = 2$. These two figures show the differences relative to the results for $m = 0$ and $\Delta E/E_b = 0$, respectively. The negative relative reference indicates that the non-homogeneity causes the minimum Re[λ] to be smaller than that for a homogeneous plate. It is interesting to note that the minimum values of Re[λ] for the vertex angle equal to 180°, 270° and 360° are not affected by material non-homogeneity. When the vertex angle is between around 120° and 180° or between 270° and 360°, the material non-homogeneity yields the minimum Re[λ] smaller than that for a homogeneous plate. The opposite trend is observed when the vertex angle is between 180° and 270°. Increasing the value of m does not necessarily decrease the relative differences; however, increasing the value of $\Delta E/E_b$ enlarges the relative differences.

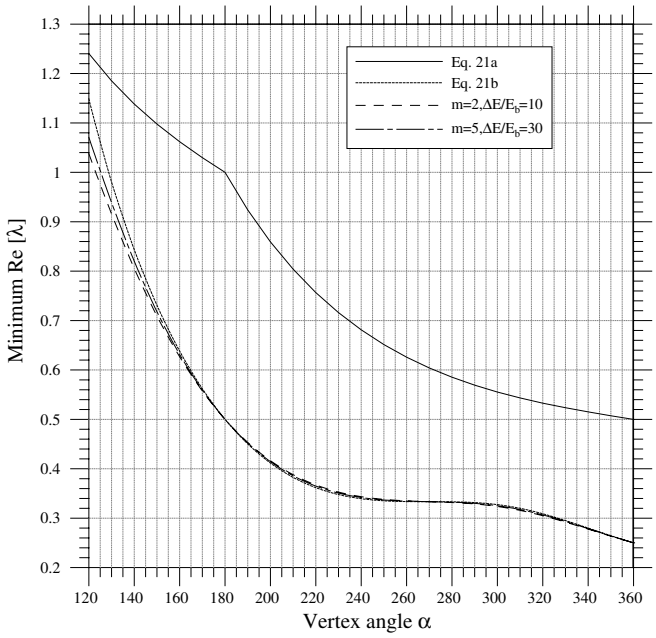

Fig. 4. Minimum Re[λ] of characteristic equations corresponding to simply supported-clamped boundary condition.

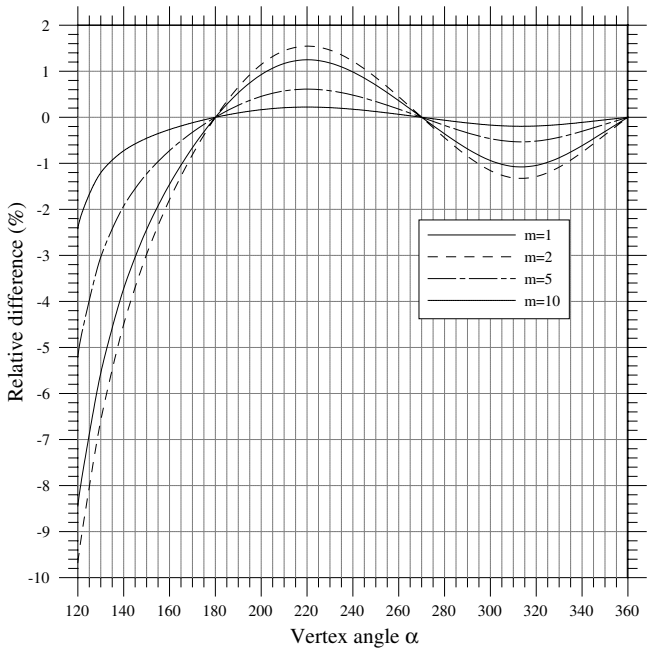

Fig. 5. The effects of m on minimum Re[λ] of the characteristic equation corresponding to simply supported–clamped boundary condition.

Figs. 7–9 present the effects of material non-homogeneity on the minimum Re[λ] of the characteristic equation corresponding to simply supported-free boundary condition. When $m = 0$ or $\Delta E = 0$, the following characteristic equations are obtained:

$$-4 + \lambda^2(1+\upsilon)^2 \sin^2\alpha - (-3+\upsilon)(1+\upsilon)\sin^2\lambda\alpha = 0 \tag{22a}$$

$$\text{or } -\lambda(-1+\upsilon)\sin 2\alpha + (3+\upsilon)\sin 2\lambda\alpha = 0. \tag{22b}$$

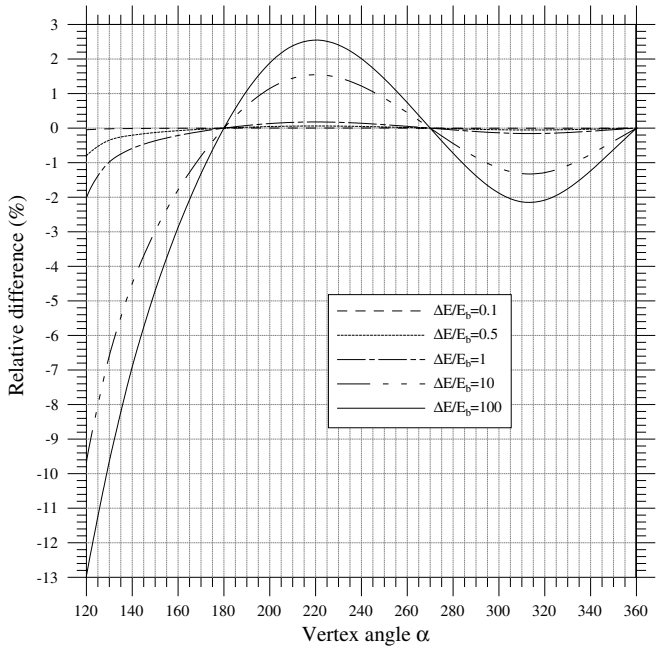

Fig. 6. The effects of $\Delta E/E_b$ on minimum Re[λ] of the characteristic equation corresponding to simply supported–clamped boundary condition.

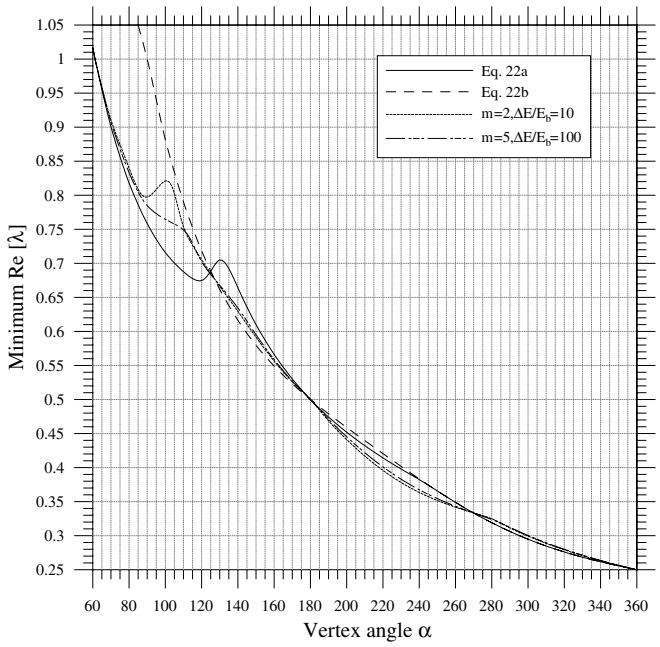

Fig. 7. Minimum Re[λ] of characteristic equations corresponding to simply supported–free boundary condition.

Eq. (22a) is identical to the characteristic equation for a homogeneous wedge with fixed-free boundary condition under extension (Williams, 1952a). Eq. (22b) is the same as the characteristic equation for a homogeneous wedge with simply supported and free radial edges under bending (Williams, 1952b). Fig. 7 presents the minimum Re[λ] for Eqs. (22a) and (22b). The differences relative to the results for $m = 0$ and $\Delta E/E_b = 0$ are shown in Figs. 8 and 9, respectively. The value of $\Delta E/E_b$ is 10 in Fig. 8, and $m = 2$ in Fig. 9.

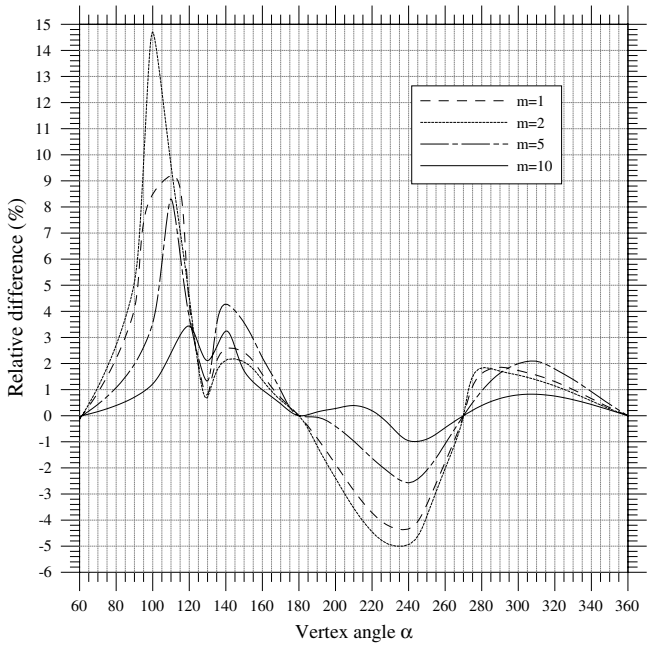

Fig. 8. The effects of m on minimum Re[λ] of the characteristic equation corresponding to simply supported–free boundary condition.

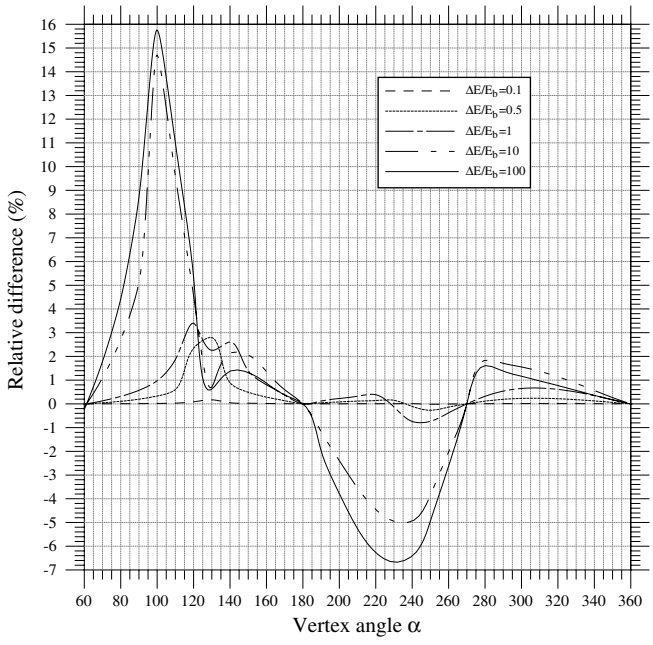

Fig. 9. The effects of $\Delta E/E_b$ on minimum Re[λ] of the characteristic equation corresponding to simply supported–free boundary condition.

Figs. 7–9 reveal several facts. Depending on the vertex angle, the minimum Re[λ] of Eq. (22a) can be larger or smaller than that of Eq. (22b). When the vertex angle is smaller than 126.4°, the stress singularities caused by extension are more severe than those produced by bending. Changing m or $\Delta E/E_b$ does not affect the minimum Re[λ] when the vertex angle is 180°, 270°, or 360°. When the vertex angle is between around 61° and 180°or between 270° and 360°, the material non-homogeneity yields a minimum Re[λ] larger than that for

a homogeneous plate. Increasing m or $\Delta E/E_b$ does not always enlarge the difference between the minimum $\mathrm{Re}[\lambda]$ for an FGM plate and that for a homogenous plate.

6. Concluding remarks

This study has developed the equilibrium equations in terms of displacement functions for an FGM thin plate based on the classical plate theory and established the asymptotic displacement field to describe the singular behaviors of stress resultants in the vicinity of a sharp corner. The asymptotic solutions were obtained using the eigenfunction expansion method and assuming non-homogeneous Young's modulus and constant Poisson ratio along plate thickness. This work has also established the characteristic equations for determining stress singularity orders at the vertex of the corner with different boundary condition combinations. These asymptotic solutions and characteristic equations are the first given in the literature. Only the characteristic equations corresponding to boundary conditions involving simple support depend on material non-homogeneity. Nevertheless, regardless of the boundary conditions considered, the asymptotic solutions of in-plane and out-of-plane displacement components on the mid-plane are usually coupled when $\overline{E}_1 \neq 0$, as defined in Eq. (5).

In examining how material non-homogeneity affects stress singularity orders, this work considered the non-homogeneous Young's modulus following a power law. The dominant stress singularities due to a simply supported-simply supported boundary condition are very likely independent of the material non-homogeneity. When the simply supported-clamped boundary condition around a corner is considered, the material non-homogeneity increases the stress singularity strength when the vertex angle is between approximately 120° and 180° or between 270° and 360°; and an opposite trend is observed when the vertex angle is between 180° and 270°. When a simply supported-free boundary condition is considered, the material non-homogeneity decreases the stress singularity strength when the vertex angle is between approximately 61° and 180° or between 270° and 360°.

The corner functions shown here will be utilized in future FGM plate studies involving geometrically induced stress singularities to determine accurate free vibration frequencies and mode shapes of thin plates having such boundary discontinuities. Because other corner functions have been used advantageously for vibration studies of homogeneous plates (Huang et al., 2005), the present corner functions are definitely appropriate for FGM thin plate vibration problems. These corner functions can also be used for static stress and deformation analysis, especially for determining the stress intensity factors for a V-notch or a crack.

Acknowledgement

This work reported herein was supported by the National Science Council, R.O.C. through research Grant No. NSC94-2211-E-009-011. This support is gratefully acknowledged.

References

Bažant, Z.P., Estenssoro, L.F., 1977. General numerical method for three-dimensional singularities in cracked or notched elastic solids. In: Proceedings of the 4th International Conference on Fracture, Eaterloo, Ontario, vol. 3, pp. 371–385.

Bogy, D.B., 1971. Two edge-bonded elastic wedges of different materials and wedge angles under surface tractions. Journal of Applied Mechanics 38 (2), 377–386.

Burton, W.S., Sinclair, G.B., 1986. On the singularities in Reissner's theory for the bending of elastic plates. Journal of Applied Mechanics 53, 220–222.

Chen, J., Wu, L., Du, S., 2000. Modified J integral for functionally graded materials. Mechanics Research Communications 27, 301–306.

Delale, F., Erdogan, F., 1983. The crack problem for a nonhomogeneous plane. Journal of Applied Mechanics 50, 609–614.

Delale, F., Erdogan, F., 1988. Interface crack in a nonhomogeneous elastic medium. International Journal of Engineering Science 26, 559–568.

Dempsey, J.P., Sinclair, G.B., 1981. On the singular behavior at the vertex of a bi-material wedge. Journal of Elasticity 11 (3), 317–327.

Erdogan, F., 1985. The crack problem for bonded nonhomogeneous material under antiplane shear loading. Journal of Applied Mechanics 52, 823–828.

Erdogan, F., Kaya, A.C., Joseph, P.F., 1991. The crack problem in bonded nonhomogenous materials. Journal of Applied Mechanics 58, 410–418.

Gdoutos, E.E., Theocaris, P.S., 1975. Stress concentrations at the apex of a plane indenter acting on an elastic half-plane. Journal of Applied Mechanics 42 (3), 688–692.
Ghahremani, F., 1991. A numerical variational method for extracting 3D singularities. International Journal of Solids and Structures 27 (11), 1371–1386.
Glushkov, E., Glushkova, N., Lapina, O., 1999. 3-D elastic stress singularity at polyhedral corner points. International Journal of Solids and Structures 36 (8), 105–1128.
Gu, P., Asaro, R.J., 1997. Crack deflection in functionally graded material. International Journal of Solids and Structures 34, 3085–3098.
Gu, P., Dao, M., Asaro, R.J., 1999. A simplify method for calculating the crack-tip field for functionally graded materials using the domain integral. Journal of Applied Mechanics 66, 101–108.
Hein, V.L., Erdogan, F., 1971. Stress singularities in a two-material wedge. International Journal of Fracture Mechanics 7 (3), 317–330.
Huang, C.S., 2002a. Corner singularities in bi-material Mindlin plates. Composite Structures 56, 315–327.
Huang, C.S., 2002b. On the singularity induced by boundary conditions in a third-order thick plate theory. Journal of Applied Mechanics 69, 800–810.
Huang, C.S., 2003. Stress singularities at angular corners in first-order shear deformation plate theory. International Journal of Mechanical Science 45 (1), 1–20.
Huang, C.S., 2004. Corner stress singularities in a high-order plate theory. Computers & Structures 82, 1657–1669.
Huang, C.S., Leissa, A.W., in press. Three-dimensional sharp corner displacement functions for bodies of revolution. Journal of Applied Mechanics.
Huang, C.S., Leissa, A.W., Chang, M.J., 2005. Vibrations of skewed cantilevered triangular, trapezoidal and parallelogram Mindlin plates with considering corner stress singularities. International Journal for Numerical Methods in Engineering 62, 1789–1806.
Jin, Z.–H., Dodds Jr., R.H., 2004. Crack growth resistance behavior of a functionally graded material: computational studies. Engineering Fracture Mechanics 71, 1651–1672.
Jin, Z.-H., Noda, N., 1993. Minimization of thermal stress intensity factors for a crack in a metal–ceramic mixture. In: Ceramic Transactions. In: Holt, J.B. et al. (Eds.), vol. 34: Functionally Gradient Materials. The American Ceramic Society, Westerville, OH, pp. 47–54.
Keer, L.M., Parihar, K.S., 1977. Singularity at the vertex of pyramidal notches with three equal angles. Quarterly Journal of Applied Mathematics 35 (2), 401–405.
Kim, J.H., Paulino, G.H., 2002. Mixed-mode fracture of orthotropic functionally graded materials using finite element and the modified crack closure method. Engineering Fracture mechanics 69, 1557–1586.
Leissa, A.W., McGee, O.G., Huang, C.S., 1993. Vibrations of sectorial plates having corner stress singularities. Journal of Applied Mechanics 60, 134–140.
McGee, O.G., Kim, J.W., Leissa, A.W., 2005. Sharp corner functions for Mindlin plates. Journal of Applied Mechanics 72 (1), 1–9.
Müller, D.E., 1956. A method for solving algebraic equations using an automatic computer. Mathematical Tables and Aids to Computation 10, 208–215.
Niino, M., Maeda, S., 1990. Recent development status of functionally gradient materials. ISIJ International 30 (9), 699–703.
Noda, N., Jin, Z.–H., 1993. Thermal stress intensity factors for a crack in a strip of a functionally gradient material. International Journal of Solids and Structures 30, 1039–1056.
Rao, A.K., 1971. Stress concentrations and singularities at interface corners. Zeitschrift fur Angewandte Mathematik und Mechanik 51, 395–406.
Reddy, J.N., 1999. Theory and Analysis of Elastic Plates. Taylor & Francis, London.
Rousseau, C.-E., Tippur, H.V., 2002. Evaluation of crack tip fields and stress intensity factors in functionally graded elastic materials: crack parallel to elastic gradient. International Journal of Fracture 114, 87–111.
Schmitz, H., Volk, K., Wendland, W., 1993. Three-dimensional singularities of elastic fields near vertices. Numerical Methods for Partial Differential Equations 9 (3), 323–337.
Somaratna, N., Ting, T.C.T., 1986. Three-dimensional stress singularities in anisotropic materials and composites. International Journal of Engineering Science 24 (7), 1115–1134.
Ting, T.C.T., Chou, S.C., 1981. Edge singularities in anisotropic composites. International Journal of Solids and Structures 17 (11), 1057–1068.
Williams, M.L., 1952a. Stress singularities resulting from various boundary conditions in angular corners of plates in extension. Journal of Applied Mechanics 19, 526–528.
Williams, M.L., 1952b. Surface stress singularities resulting from various boundary conditions in angular corners of plates under bending. In: Proceedings of the First US National Congress of Applied Mechanics, pp. 325–329.
Yue, Z.Q., Xiao, H.T., Tham, L.G., 2003. Boundary element analysis of crack problems in functionally graded materials. International Journal of Solids and Structures 40, 3273–3291.